

Activation of long non-coding RNA NEAT1 leads to survival advantage of multiple myeloma cells by supporting a positive regulatory loop with DNA repair proteins

Elisa Taiana,^{1,2} Cecilia Bandini,^{3,4} Vanessa Katia Favasuli,^{1,2} Domenica Ronchetti,^{1,2} Ilaria Silvestris,^{1,2} Noemi Puccio,^{1,2} Katia Todoerti,¹ Silvia Erratico,^{5,6} Domenica Giannandrea,⁷ Niccolò Bolli,^{1,2} Nicola Amodio,⁸ Alessia Ciarrocchi,⁹ Raffaella Chiaramonte,⁷ Yvan Torrente,⁶ Roberto Piva^{3,4} and Antonino Neri^{1,2*}

¹Hematology, Fondazione Cà Granda IRCCS Policlinico, Milan; ²Department of Oncology and Hemato-oncology, University of Milan, Milan; ³Department of Molecular Biotechnology and Health Sciences, University of Turin, Turin; ⁴Città Della Salute e della Scienza Hospital, Turin; ⁵Novystem Spa, Milan; ⁶Stem Cell Laboratory, Department of Pathophysiology and Transplantation, University of Milan, Centro Dino Ferrari, Unit of Neurology, Fondazione Cà Granda IRCCS Policlinico, Milan; ⁷Department of Health Sciences, University of Milan, Milan; ⁸Department of Experimental and Clinical Medicine, Magna Graecia University of Catanzaro, Catanzaro and ⁹Laboratory of Translational Research, Azienda Unità Sanitaria Locale-IRCCS Reggio Emilia, Reggio Emilia, Italy

*Current address: Scientific Directorate, Azienda USL-IRCCS Reggio Emilia, Italy

Correspondence: E. Taiana

elisa.taiana@unimi.it

A. Neri

antonino.neri@unimi.it

Received: March 31, 2022.

Accepted: September 1, 2022.

Prepublished: September 8, 2022.

<https://doi.org/10.3324/haematol.2022.281167>

©2023 Ferrata Storti Foundation

Published under a CC BY-NC license



SUPPLEMENTARY DATA

Supplementary Methods

Lentivirus production and in vitro transduction

High titer lentiviral stocks were produced in 293T cells by co-transfecting expression vectors, packaging and envelope vectors (psPAX2 and pMD2.G) with the Effectene Transfection Reagent (Qiagen, Germantown MD 20874, USA), according to the manufacturer's instructions. Supernatants were harvested over 36 to 60 hours, filtrated (0.22 μm pore), and used directly or concentrated by ultracentrifugation at 4°C, for 2 h at 50,000 rcf, and then resuspended in cold phosphate-buffered saline (PBS). Aliquots of virus, plus 4-8 $\mu\text{g}/\text{mL}$ polybrene, were used to infect AMO-1 cells ($1 \times 10^5/\text{mL}$). Fresh medium was supplemented 4 h after infection. Stable cell lines expressing indicated constructs were selected by treatment with blasticidin or hygromycin for 5 or 6 days.

Plasmids constructs and cloning of sgRNAs

To induce NEAT1 transactivation, the plasmids lenti sgRNA(MS2)_puro backbone, lenti dCAS9-VP64_Blast, and lenti MS2-p65-HSF1_Hygro were obtained from Addgene (<http://www.addgene.org/>). sgRNAs targeting NEAT1 promoter region were selected from CRISPRi library of Tomohiro Yamazaki [Yamazaki, T., Biochemical and biophysical research communications 2018].

To maximize on target and minimize off target activities, three top-ranking candidate gRNA sequences were selected. Sequences were cloned via BsmBI site into lenti sgRNA(MS2)_puro backbone. The vector was digested with BsmBI, purified with a QIAquick Gel Extraction Kit (Qiagen) and dephosphorylated. Equal amount (100 μM) of complementary oligonucleotide was mixed in T4 DNA ligase buffer with T4 polynucleotide kinase (PNK) enzyme for annealing and phosphorylation. These annealed seed pairs were ligated into the BsmBI-digested lentiviral vector using T4 ligase. The ligation mixture was transformed into Stab13 competent cells. Positive clones were identified by Sanger sequencing.

Reverse transcription and quantitative PCR

Total RNA was extracted using TRIzol® Reagent (Invitrogen, Life Technologies) according to the manufacturer's instructions. The purity and concentration of total RNA were determined by the NanoDrop 1000 spectrophotometer (Thermo Fisher Scientific). The ratios of absorption (260 nm/280 nm) of all samples were between 1.8 and 2.0. cDNA was synthesized from 500 ng of total RNA with random primers using the High Capacity cDNA Reverse Transcriptase Kit (Invitrogen) according to the manufacturer's instructions. To evaluate the expression levels of listed genes, RT-PCR was performed using SYBR green PCR Master Mix (Applied Biosystems) after optimization of the primer conditions. 10 ng of reverse-transcribed RNAs were mixed with 300 nM of specific forward and reverse primers in a final volume of 10 µl. RT-PCR was performed on an Applied Biosystems StepOnePlus Real-Time PCR system for 40 cycles. Data were analyzed using the $2^{-\Delta Ct}$ method or the $2^{-\Delta\Delta Ct}$ method to measure the relative changes in each gene's expression compared with GAPDH expression. To determine RNA levels by qPCR, the following primers were used:

Primer	Sequence (5' - 3')
Total NEAT1_Fw	5' - GCCTTG TAGATGGAGCTTGC - 3'
Total NEAT1_Rw	5' - GCACAACACAATGACACCCT - 3'
NEAT1_2_Fw	5' - GGCCAGAGCTTTGTTGCTTC - 3'
NEAT1_2_Rw	5' - GGTGCGGGCACTTACTTACT - 3'
GAPDH_Fw	5' - ACAGTCAGCCGCATCTTCTT - 3'
GAPDH_Rw	5' - AATGAAGGGGTCATTGATGG - 3'
NONO_Fw	5' - AACATCAAGGAGGCTCGTGA - 3'
NONO_Rw	5' - GTCGCCGCATCATTTCTTCT - 3'
SFPQ_Fw	5' - CGGAGGAGCAATGAACATGG - 3'
SFPQ_Rw	5' - AGTACGCATGTCACTTCCCA - 3'
FUS_Fw	5' - TGGAACTCAGTCAACTCCCC - 3'
FUS_Rw	5' - CTGCTACCGTAACTTCCCGA - 3'
RPA2_Fw	5' - CGTTTGTGGTGCCAGAGAAA - 3'
RPA2_Rw	5' - TTTTCGGCTTGAGAAGGTGC - 3'
ATM_Fw	5' - AGGCCGGAAGATGAAACTGA - 3'
ATM_Rw	5' - TGGGAAAAGTCGGCTGAGAT - 3'
ATR_Fw	5' - ACAGAGCCAAGGAGCCTATC - 3'
ATR_Rw	5' - GTTCAGCGAGTCGTGATTCC - 3'

Primer	Sequence (5' - 3')
PRKDC_Fw	5' - CTGTGTGAACTGGTTGCGAA - 3'
PRKDC_Rw	5' - TCATTCCCTCCACACGACAA - 3'

Colony-forming assay

For colony-forming assay, AMO-1^{SAM} cells were suspended in RPMI-1640 medium with 1% or 10% fetal bovine serum (FBS) and plated on methylcellulose-based media (MethoCult™ STEMCELL Technologies, Italy) containing 1% methylcellulose in RPMI-1640 medium. Each condition was evaluated twice in triplicates. Colonies, defined as aggregates greater than or equal to 50 cells, were scored by an inverted microscope after incubation at 37 °C in a fully humidified atmosphere at 5% CO₂.

Cell cycle analysis and apoptosis

Cell cycle distribution of AMO-1^{SAM} cells was assessed using BD FACSVerse™ flow cytometer (BD Bioscience, Italy). Samples for cell cycle analysis were fixed in 70% ethanol at 4 °C for at least 2 h and incubated with FxCycle™ PI/RNase Staining Solution (Life Technologies, Italy) for 30 min in the dark, according to the manufacturer's instructions. Fluorescent emissions were collected through a 575 nm band-pass filter. To detect apoptosis, cells were harvested, washed twice, and suspended in binding buffer. Then, the cells were stained using a PE Annexin V Apoptosis Detection Kit (BD Biosciences), following which they were subjected to BD FACSVerse™ flow cytometry (BD Biosciences) to analyze apoptotic distribution.

Immunofluorescence

0.1 x 10⁶ cells were harvested, centrifuged onto glass slides (Cytospin 4, Thermo Scientific), then fixed in 4% paraformaldehyde in PBS1X for 12 min at 22°C, followed by three 5-min washes in PBS. Cells were permeabilized (0.1% Triton X-100 in PBS, 15-min), washed in PBS (3X, 5 min

each), blocked 1 h at 22°C with 1.5% BSA in PBS, and then incubated 1 hour at 4°C with specific primary antibodies (1:200).

Thereafter, slides incubated with primary antibody specific for NONO were washed three times in PBS and mounted under coverslips with DAPI-containing Vectashield (Vector Laboratories). Slides incubated with primary antibody specific for DNA-PKcs and pRPA32 were washed in PBS (3X, 5 min each), and incubated 1 h at 22°C in the dark, with secondary Antibody (listed below). After three PBS washes, cells were mounted under coverslips with DAPI-containing Vectashield (Vector Laboratories). Images were acquired by Leica TCS SP8 confocal laser scanning microscope (DMi8); acquisitions were performed with 40X and 63X immersion oil objectives. Conversion of imaged z-stacks into average intensity projections was processed by Leica Microsystem software (Leica Application Suite X - LAS X).

Protein	Ab Cod.		Source	Application
NONO (nmt55 / p54nrb)	ab208404	Abcam	Alexa Fluor 488-conjugated	IF
pRPA32 (S4/S8)	ab264116	Abcam	Rabbit pAb	IF
DNA-PKcs	#12311	Cell Signaling	Mouse mAb	IF
Anti-mouse IgG	#4408	Cell Signaling	Alexa Fluor 488	IF
Anti-rabbit IgG	#4413	Cell Signaling	Alexa Fluor 555	IF

RNA FISH

RNA FISH was performed to evaluate the expression of NEAT1. We used the Stellaris RNA FISH kit (Biosearch Technologies), according to the manufacturer's instructions. For NEAT1 detection, we took advantage of a commercial set of Quasar® 570-labeled oligos (Stellaris, Biosearch Technologies) able to bind the 5' end of NEAT1 transcript. Images were acquired by Leica TCS SP8 confocal laser scanning microscope (DMi8); acquisitions were performed with 40X and 63X oil immersion objectives. Conversion of imaged z-stacks into average intensity projections was processed by Leica Microsystem software (Leica Application Suite X - LAS X).

Proteomic assays

Cells were homogenized in lysis buffer M-PER® Mammalian Protein Extraction Reagent (Thermo Scientific, Italy) and Halt Protease and Phosphatase inhibitor cocktail, EDTA-free, 100X, (Thermo Scientific). Whole cell lysates (40 µg per cell line) from AMO-1^{N#8}, AMO-1^{N#5}, and AMO-1^{SCR} cell lines were separated using Bolt™ 4-12% Bis-Tris Plus Acrylamide Gels (Invitrogen), electro-transferred onto nitrocellulose membranes (Bio-Rad, Hercules, CA, USA), and immunoblotted with specific primary antibody (listed below). Membranes were washed three times in PBST solution and then incubated with a secondary antibody conjugated with horseradish peroxidase (HRP) in BSA 2% - PBST for 2 hours at RT. Chemiluminescence was developed using Clarity ECL Western Blot Substrate Kit (BIO-RAD) and signal intensity was detected by the use of ChemiDoc MP System (Bio-Rad). The experiments were repeated at least three times.

Protein	Antibody	Source	Source	Application
NONO (nmt55 / p54nrb)	ab70335	Abcam	Rabbit pAb	WB
SFPQ	ab11825	Abcam	Mouse mAb	WB
GAPDH	sc-32233	Santa Cruz Biotechnology	Mouse mAb	WB
FUS/TLS	sc-47711	Santa Cruz Biotechnology	Mouse mAb	WB
ACTIN	A2066	Sigma-Aldrich	Rabbit	WB
pERK 1/2	M8159	Sigma-Aldrich	Mouse	WB
ERK 1/2	M5670	Sigma-Aldrich	Rabbit	WB
pAKT (S473)	#4060	Cell Signaling	Rabbit	WB
AKT	#9272	Cell Signaling	Rabbit	WB
pRPA32 (S8)	#83745	Cell Signaling	Rabbit	WB
pRPA32 (S4/S8)	ab264116	Abcam	Rabbit pAb	WB
RPA32	#52448	Cell Signaling	Rabbit	WB
pCHK2 (T68)	#2197	Cell Signaling	Rabbit mAb	WB
CHK2	#3440	Cell Signaling	Mouse mAb	WB
pCHK1 (S345)	#2348	Cell Signaling	Rabbit mAb	WB
CHK1	#2360	Cell Signaling	Mouse mAb	WB
pATR (S428)	#2853	Cell Signaling	Rabbit	WB
ATR	#13934	Cell Signaling	Rabbit mAb	WB
pATM (S1981)	#5883	Cell Signaling	Rabbit mAb	WB
ATM	#2873	Cell Signaling	Rabbit mAb	WB
DNA-PKcs	#12311	Cell Signaling	Mouse mAb	WB
CAS9	#14697	Cell Signaling	Mouse mAb	WB
NF-κB p65	#8242	Cell Signaling	Rabbit mAb	WB
Anti-mouse IgG	#7076	Cell Signaling	HRP-linked	WB
Anti-rabbit IgG	sc-2004	Santa Cruz Biotechnology	HRP-linked	WB

Inhibitors and antibiotics

The protein synthesis inhibitor Cycloheximide (100 μ M) was purchased from Selleckchem (Zürich Switzerland). DNA-PK (NU7026, 10 μ M) and ATM (KU-60019, 10 μ M) inhibitors were purchased from Selleckchem. Blastidicin (4 μ g/ml) was purchased from Gibco. Zeocin (400 μ g/ml) and Hygromycin B (200 μ g/ml) were purchased from Invitrogen. Antibiotics were added once a week to the cell culture in order to maintain the selection of infected cells.

Gymnosis

Cells were seeded at low plating density (5×10^4 cell/ml). Cells were treated for 4 days with the naked gapmeRs g#N1_E, g#N1_G and the scrambled g#SCR, at the same time of the seeding at a final concentration of 5 μ M

Name	Sequence 5'-3'	Mw, calc (Da)
g#N1_E	AGTGACCACAAAAGGT	5276.2
g#N1_G	CAAGGAAAGTCATCGC	5294.3
g#SCR	GCTCCCTTCAATCCAA	5184.2

Table S1: sequences of the three sgRNAs targeting the NEAT1 promoter of the scramble sgRNA

sgRNAs	NEAT1 sgRNA sequences (5' to 3')
g#SCR_FW	CACCGCTGAAAAGGAAGGAGTTGA
g#SCR_RW	AAACTCAACTCCTTCCTTTTCAGc
g#5_FW	CACCGCTGGGAGACCATGCACCGCC
g#5_RW	AAACGGCGGTGCATGGTCTCCAGc
g#7_FW	CACCGAGAGACTCCCGGGCGGTGCA
g#7_RW	AAACTGCACCGCCCGGGAGTCTCTc
g#8_FW	CACCGCACCGCCCGGGAGTCTCTC
g#8_RW	AAACGAGAGACTCCCGGGCGGTGC

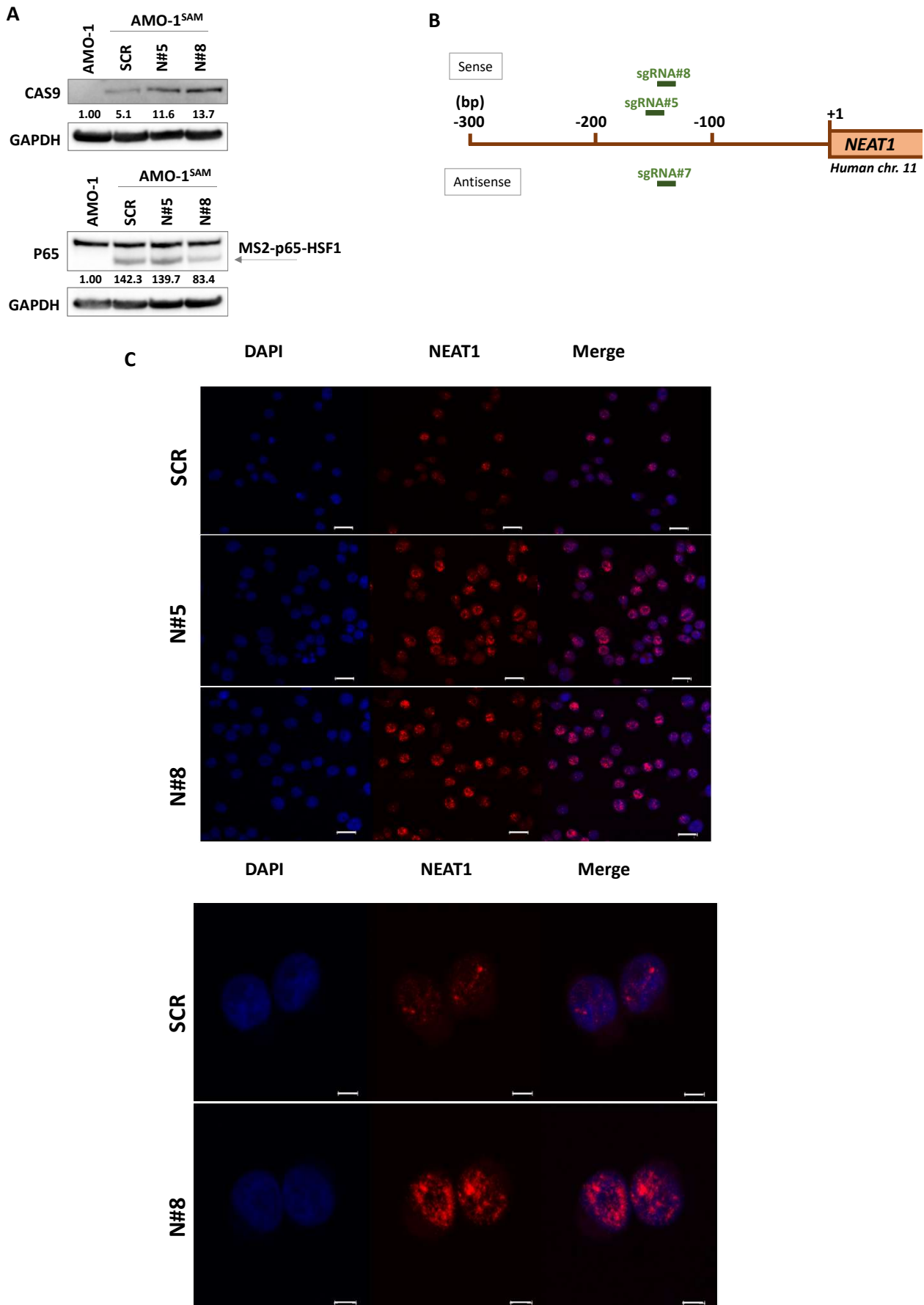


Figure S1. NEAT1 expression in AMO-1^{SAM} cells. (A) Representative WB showing Cas9 and MS2-p65-HSF1 expression in AMO-1 cells transduced with lentiviral particles expressing SAM activators. GAPDH protein expression was included for protein loading normalization. The densitometric analysis of immunoreactive bands is reported with respect to SCR condition. (B) Schematic representation of the localization of the NEAT1 specific sgRNA sequences used to engineer AMO-1 cells. (C) Confocal microscopy results of NEAT1 specific RNA-FISH in AMO-1^{SAM} cells (scale bar 20 μ m, upper panels, and 5 μ m, bottom panels).

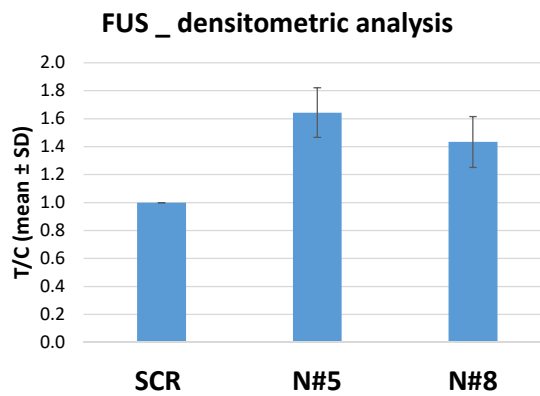
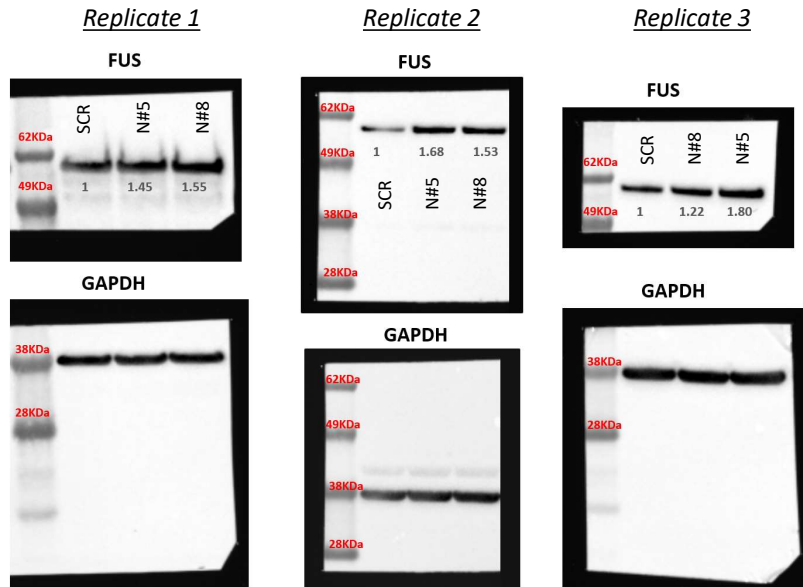


Figure S2. FUS expression in AMO-1^{SAM} cells. Three WB replicates showing FUS expression in AMO-1^{SAM} cells. GAPDH protein expression was included for protein loading normalization. The densitometric analysis of immunoreactive bands is reported with respect to SCR condition.

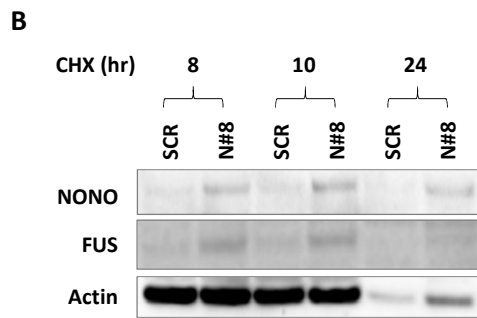
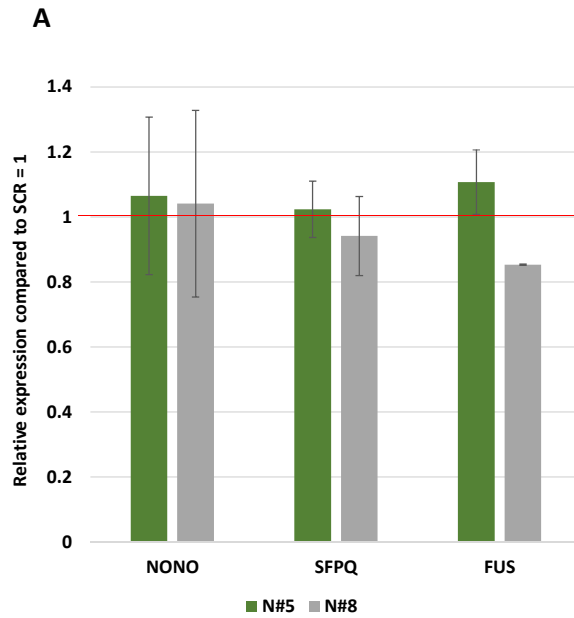


Figure S3. NEAT1 expression in AMO-1^{SAM} cells. (A) NONO, SFPQ, and FUS genes expression levels in NEAT1 transactivated AMO-1^{N#5} and AMO-1^{N#8} cells compared to scrambled controls (red line). Specific gene expression was expressed as $2^{-\Delta\Delta Ct}$ relative to the scramble condition. (B) Effect of NEAT1 transactivation in the presence of the protein synthesis inhibitor CHX (100 μ M) on the decay of NONO and FUS protein levels in AMO-1^{SCR} and AMO-1^{N#8} cells at the indicated time-point. Actin protein expression was included for protein loading normalization.

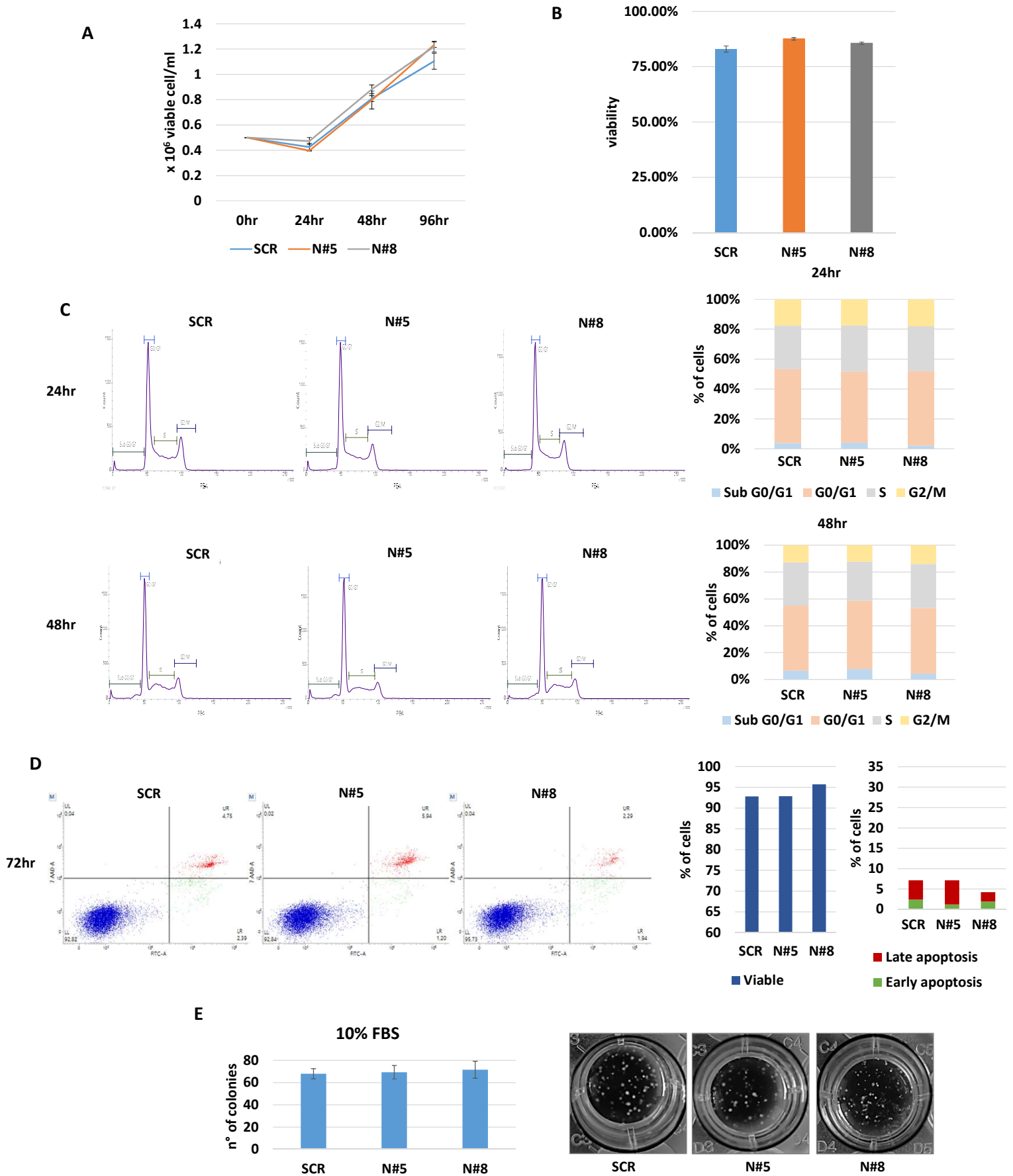


Figure S4. Analyses of AMO-1^{SAM} cells under physiological conditions (A) Growth curve of AMO-1^{SAM} cells maintained in physiological culturing condition (10% FBS, and 21% pO₂). (B) Viability of AMO-1^{SAM} after four days of cell culture. (C) Cell cycle analysis by PI staining performed in AMO-1^{SAM} cells after 24 and 48 h of culture. (D) Flow cytometry analysis of apoptosis in AMO-1^{SCR}, AMO-1^{N#5} and AMO-1^{N#8} after 72 h of culture. (E) Colony formation assay performed on AMO-1^{SAM} cultured for 14 days; representative pictures of colonies distribution at day 14 are also shown.

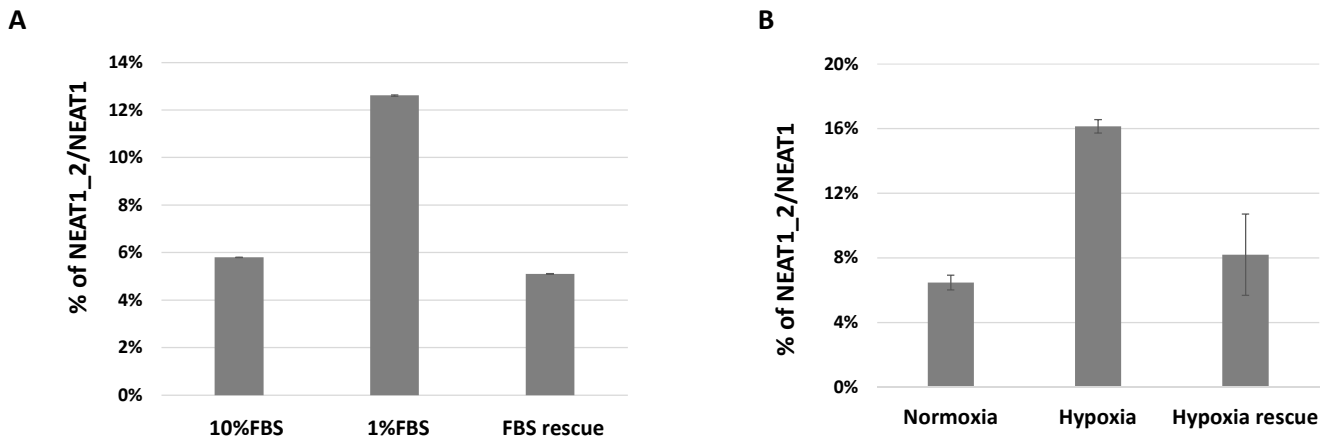


Figure S5. (A) Percentage of NEAT1_2 variant contribution respect to total NEAT1 expression in AMO-1 cells maintained for 48 h in physiological FBS culturing condition (10% FBS), in FBS starving medium, and again in physiological conditions. (B) Percentage contribution of NEAT1_2 respect to total NEAT1 expression in AMO-1 cells maintained for 48 h under normoxic or hypoxic microenvironment, and again in physiological conditions.

1% FBS

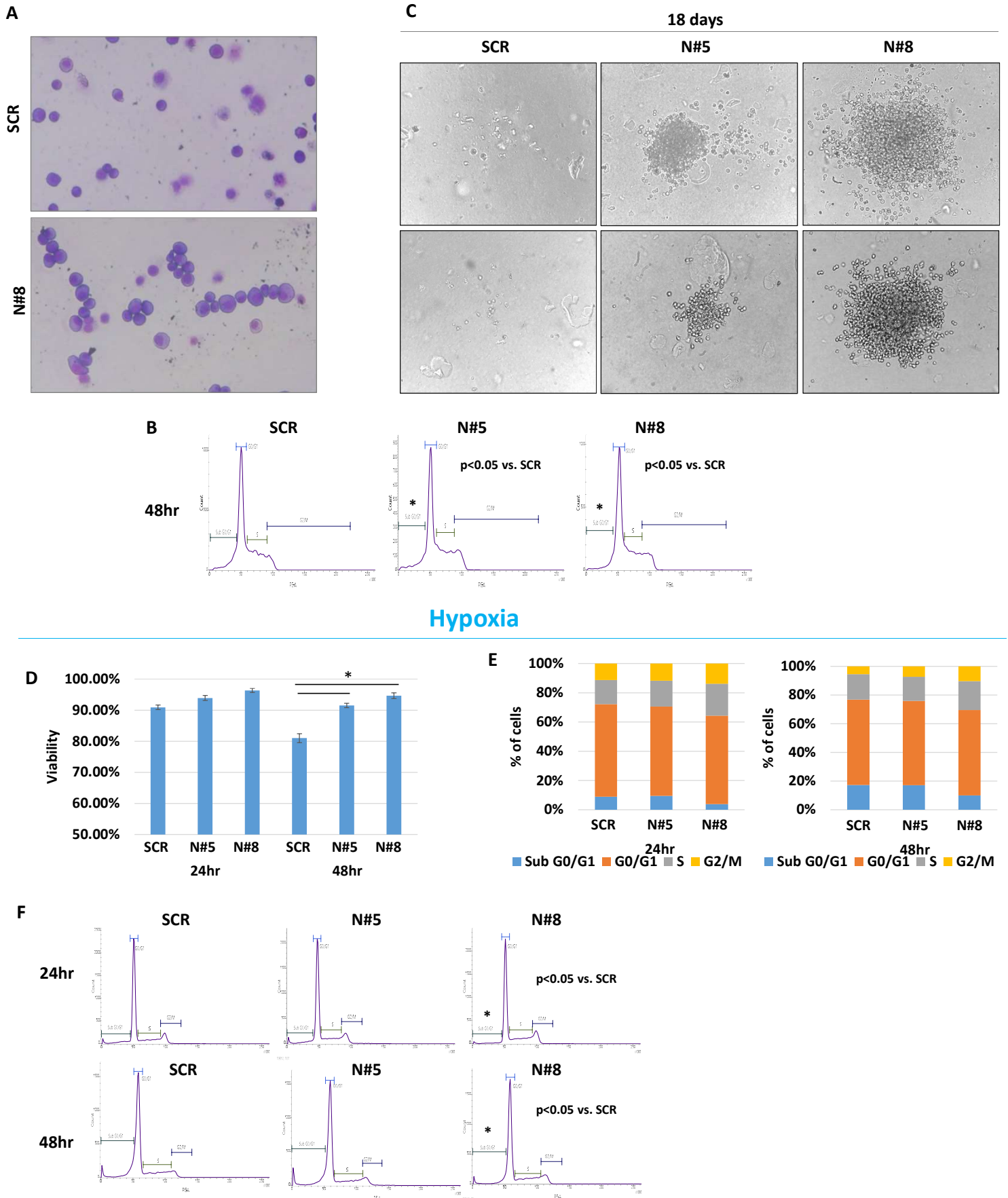


Figure S6. Analyses of AMO-1^{SAM} cells under stressful conditions. (A) Optical microscopy results obtained after May Grunwald-Giemsa (MGG) staining of AMO-1^{SCR} and AMO-1^{N#8} cells upon 48 h of culture in FBS starving condition. (B) Cell cycle analysis by PI staining in AMO-1^{SAM} cells after 48 h of FBS starving conditions. (C) Representative pictures of colony formation assay performed on AMO-1^{SAM} cultured 18 days in FBS starving condition (10x magnification). (D) Viability of AMO-1^{SAM} cells cultured for 24 h and 48 h in hypoxic condition. * p<0.05 vs. SCR. (E) Histogram of cell cycle analysis by PI staining performed in AMO-1^{SAM} cells after 24 h and 48 h of culture in hypoxic condition. (F) Cell cycle analysis by PI staining in AMO-1^{SAM} cells after 24 h and 48 h of cell culture in hypoxic conditions.

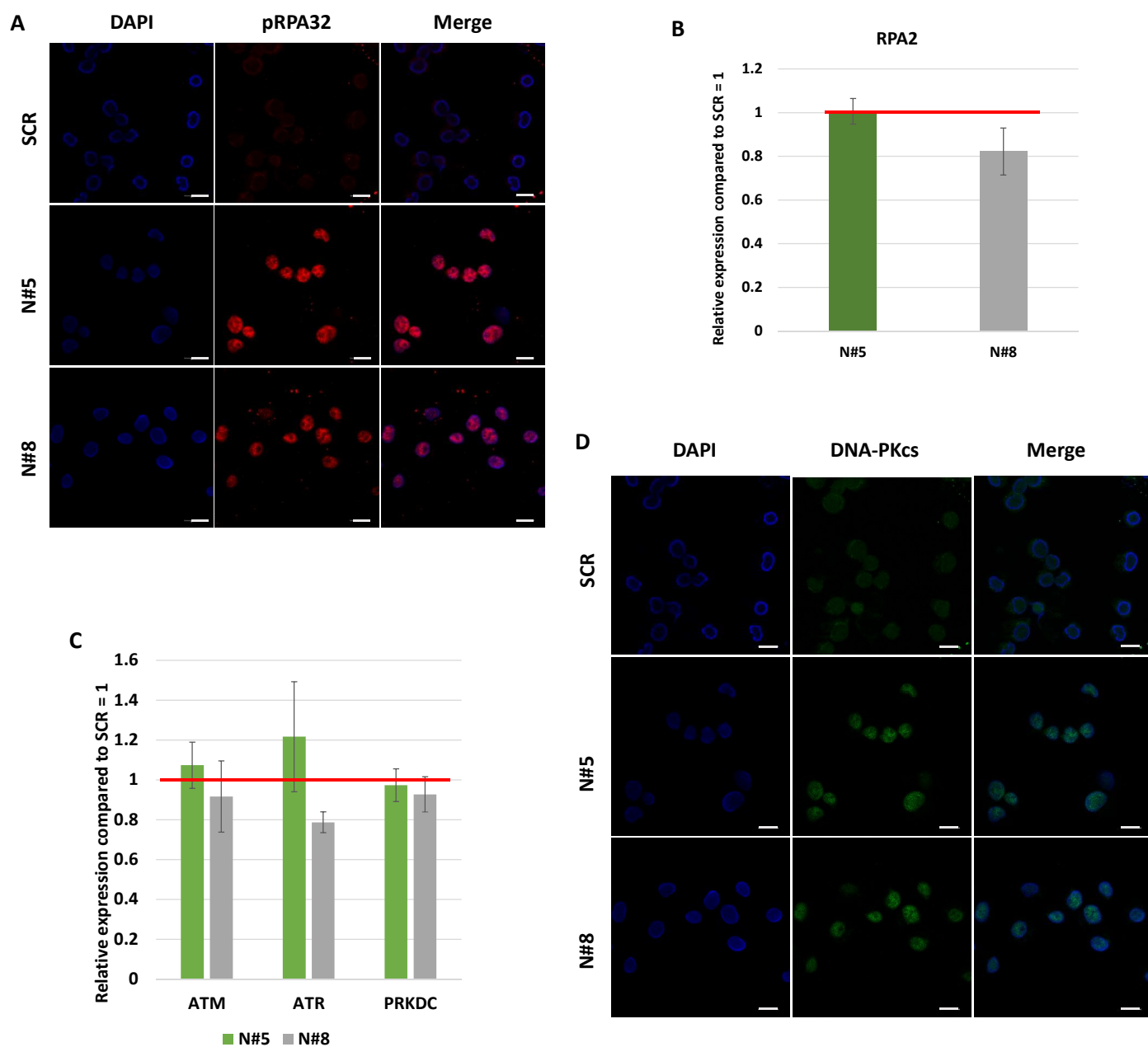


Figure S7. RPA32 and DNA-PKcs expression in AMO-1^{SAM} cells. (A) Confocal microscopy results of pRPA32 specific IF in AMO-1^{SAM} cells cultured under physiological culturing condition (scale bar 20 μ m). (B) RPA2 gene expression levels in NEAT1 transactivated AMO-1^{N#5} and AMO-1^{N#8} cells compared to scrambled controls (red line). Specific gene expression was expressed as $2^{-\Delta\Delta C_t}$ relative to the scramble condition. (C) *ATM*, *ATR*, and *PRKDC* genes expression levels in NEAT1 transactivated AMO-1^{N#5} and AMO-1^{N#8} cells compared to scrambled controls (red line). Specific gene expression was expressed as $2^{-\Delta\Delta C_t}$ relative to the scramble condition. (D) Confocal microscopy results of DNA-PKcs specific IF in AMO-1^{SAM} cells cultured under physiological culturing condition (scale bar 20 μ m).

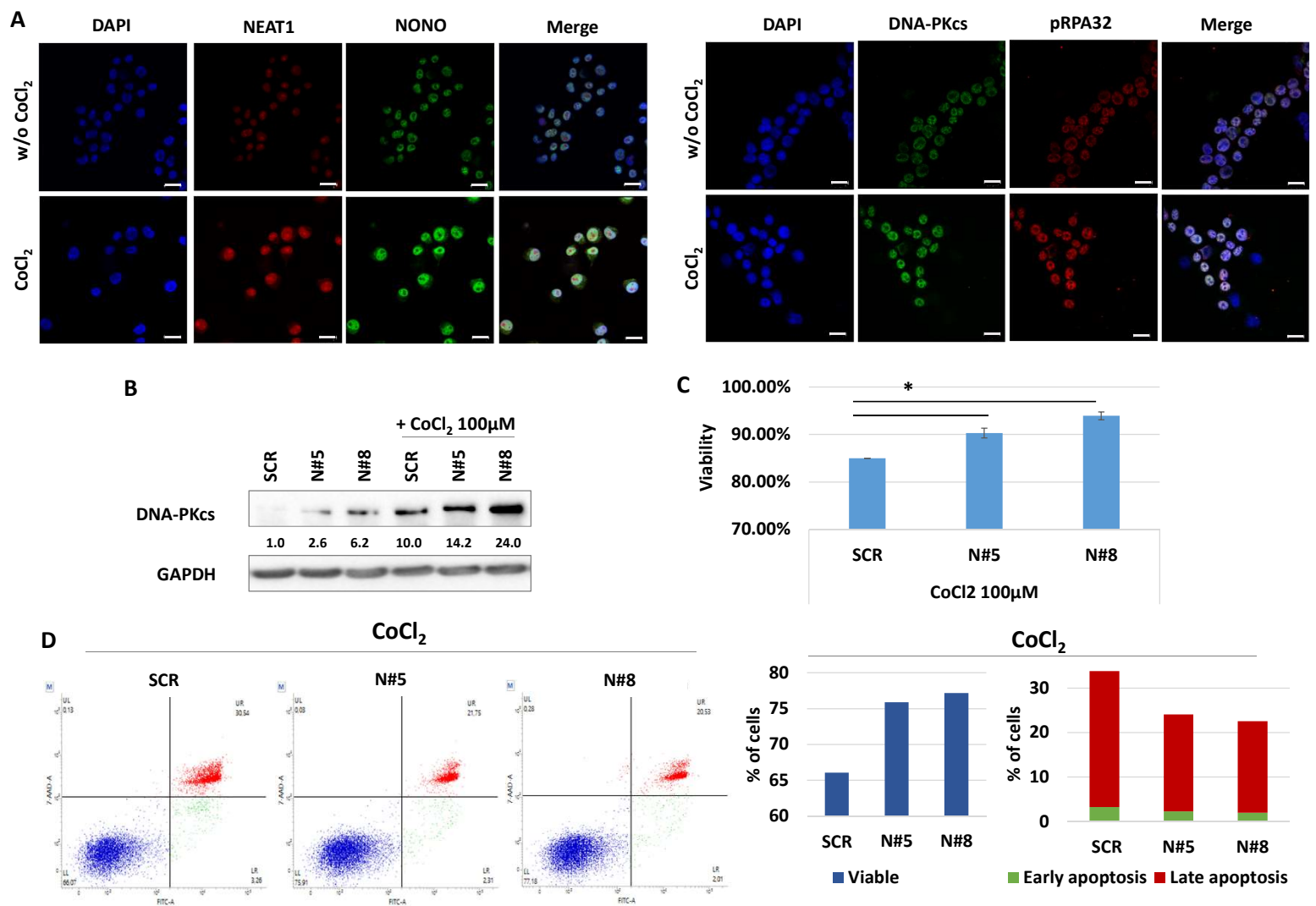


Figure S8. Effects of CoCl₂ on AMO-1^{SAM} cells. (A) confocal microscopy results of NEAT1 specific RNA-FISH and NONO IF (left panel) and confocal microscopy results of DNA-PKcs and pRPA32 specific IF (right panel) in AMO-1 cells after 48 h of culture, in the presence or absence of 100 μM CoCl₂ (for the last 24 h) (scale bar 20μm). (B) WB of DNA-PKcs in AMO-1^{SAM} cells after 48 h of culture, in the presence or absence of 100 μM CoCl₂ (for the last 24 h). GAPDH protein expression was included for protein loading normalization. The densitometric analysis of immunoreactive bands is reported with respect to SCR condition. (C) Viability of AMO-1^{SAM} after 48 h of culture, in the presence or absence of 100 μM CoCl₂ (for the last 24 h) * p<0.05 vs. SCR. (D) Flow cytometry analysis of apoptosis in AMO-1^{SCR}, AMO-1^{N#5} and AMO-1^{N#8} cultured for 48 h, in the presence or absence for the last 24 h of 100 μM CoCl₂.

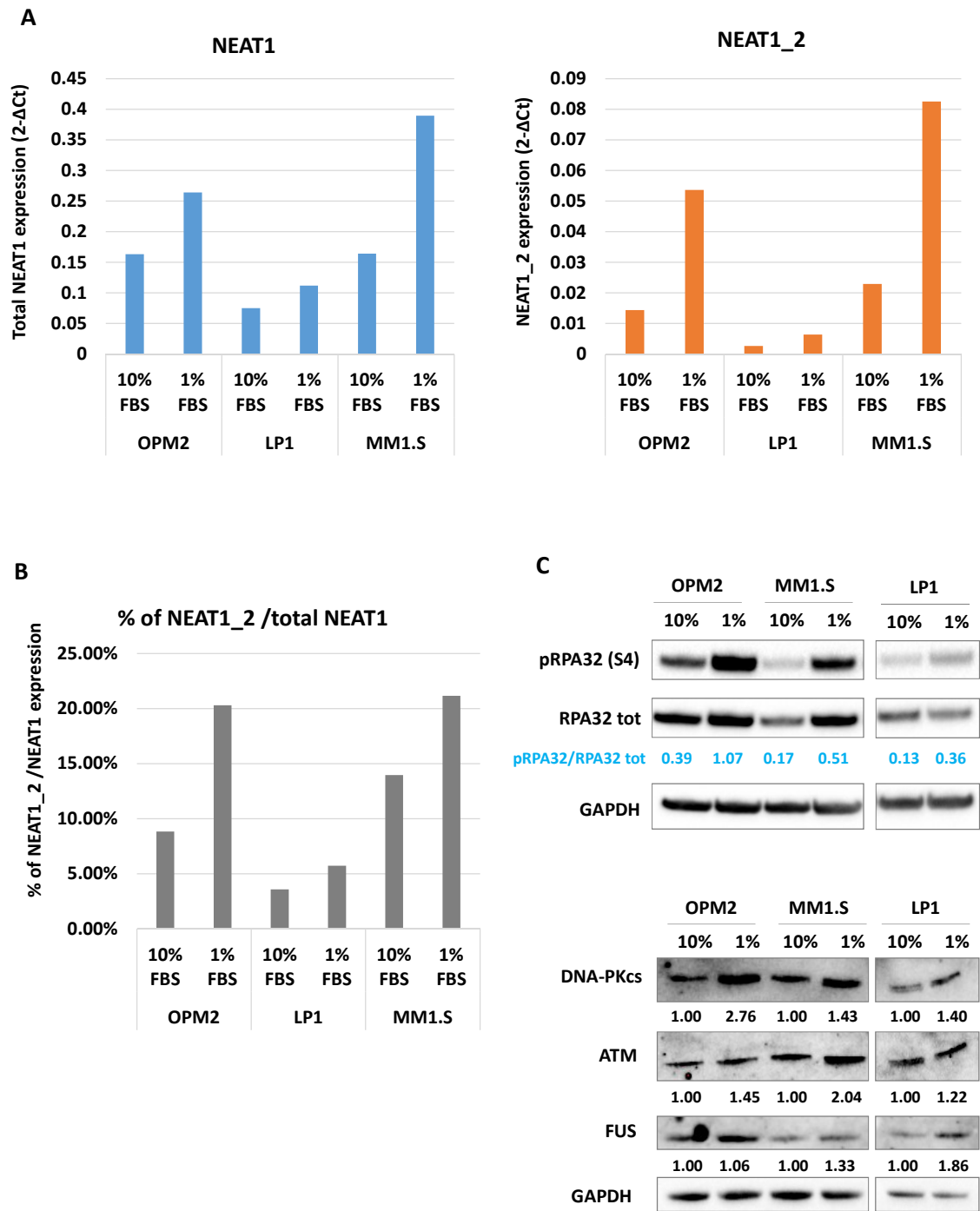


Figure S9. FBS starvation induces NEAT1-mediated molecular axis in other HMCLs. (A) qRT-PCR analyses of total NEAT1 and NEAT1_2 variant in OPM2, LP1, and MM1.S MM cells maintained for 48 h in physiological FBS culturing condition (10% FBS) and in FBS starving medium. NEAT1 expression was expressed as $2^{-\Delta Ct}$. (B) The histogram shows the percentage contribution of NEAT1_2 with respect to total NEAT1 expression in OPM2, LP1, and MM1.S MM cells cultured in FBS starving medium. (C) WB analysis of pRPA32, RPA32, DNA-PKcs, ATM, and FUS in OPM2, MM1.S, and LP1 MM cells after 48 h of culture in FBS starving condition. GAPDH protein expression was included for protein loading normalization. The densitometric analysis of immunoreactive bands is reported with respect to SCR condition.

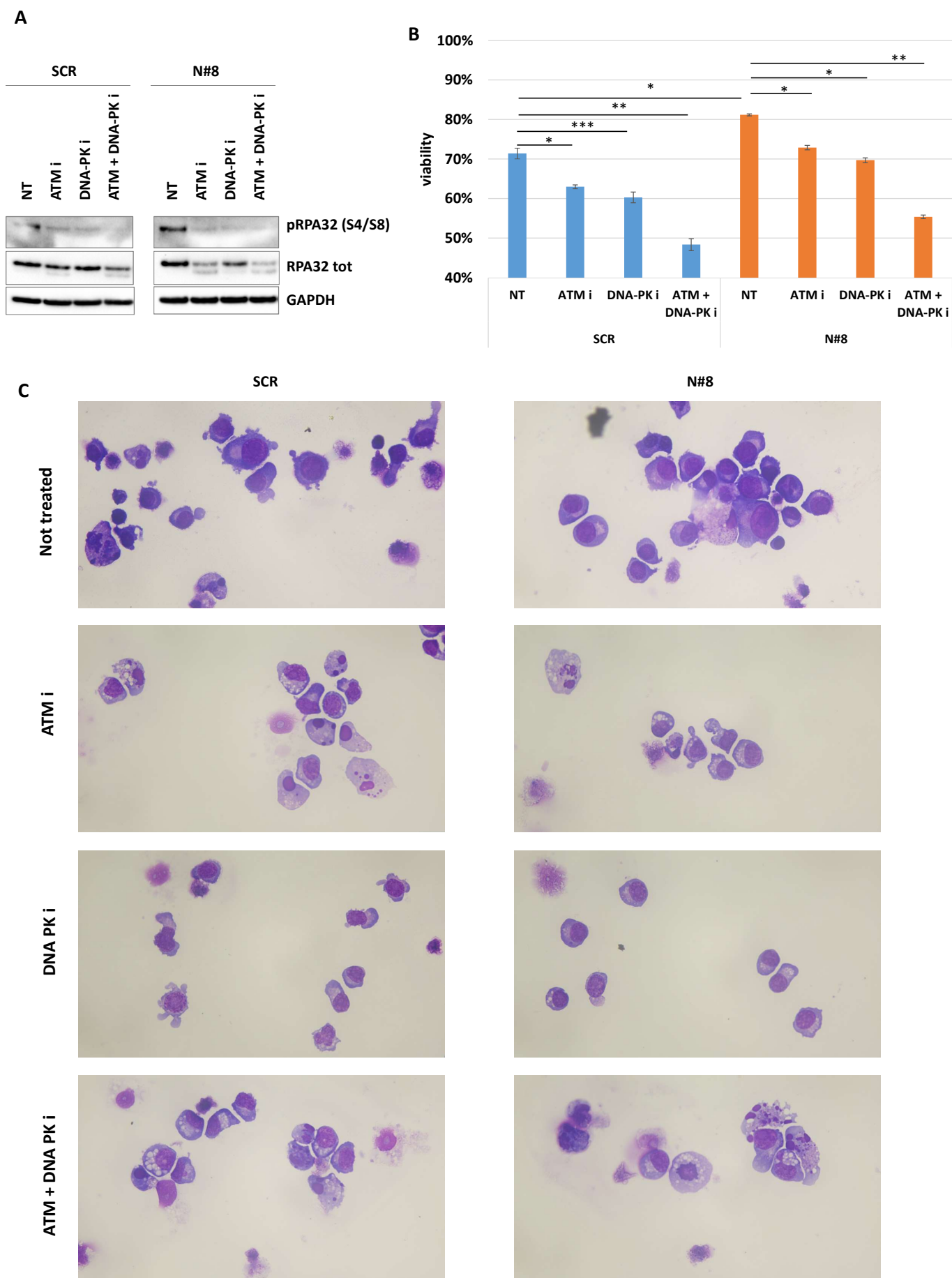


Figure S10. Effects of ATM and DNA-PK inhibitors. (A) WB analysis of pRPA32, and RPA32 in AMO-1^{SCR} and AMO-1^{N#8} cells after 24 h of ATM and DNA-PK chemical inhibition by the use of 10 μ M of KU-60019 and NU7026. GAPDH protein expression was included for protein loading normalization. (B) Viability of AMO-1^{SCR} and AMO-1^{N#8} cells after three days of culture in FBS starving condition, in the presence for the last 24 h of ATM and DNA-PK inhibitors, respectively KU-60019 and NU7026. (C) Optical microscopy results of May Grunwald-Giemsa (MGG) staining obtained in AMO-1^{SCR} and AMO-1^{N#8} cells after three days of culture in FBS starving condition, in the presence for the last 24 h of ATM and DNA-PK inhibitors. (50x magnification).

Supplementary material reporting the whole original membranes used for Figures in the manuscript and Supplementary Figures showing western blot results.
All bands, densitometry readings and molecular weight markers are reported.
SeeBlue Plus2 was used as protein ladder.
In each page, the corresponding Figure in the paper or Supplementary Figure is specified.

Figura 1B

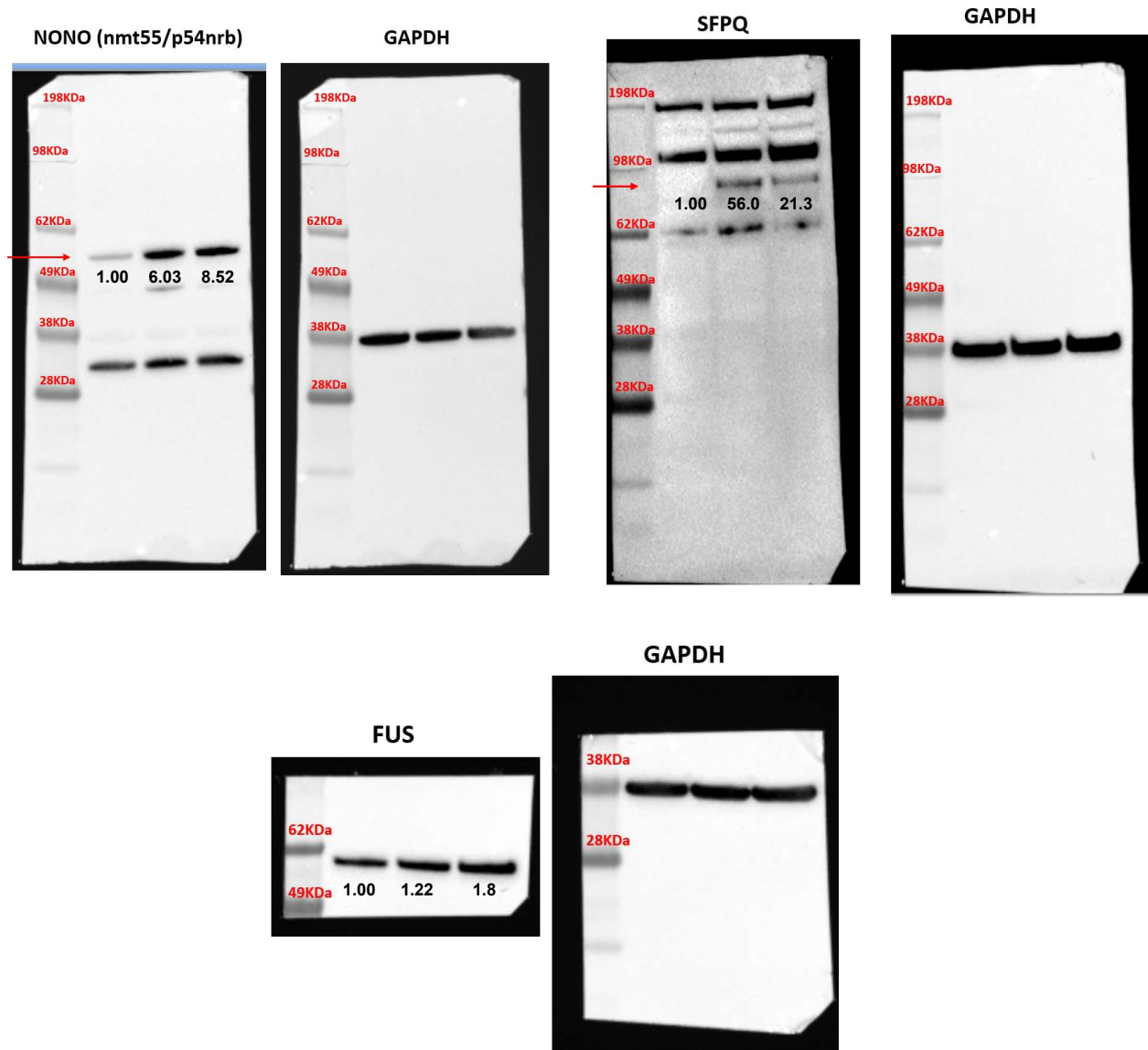


Figura 1C

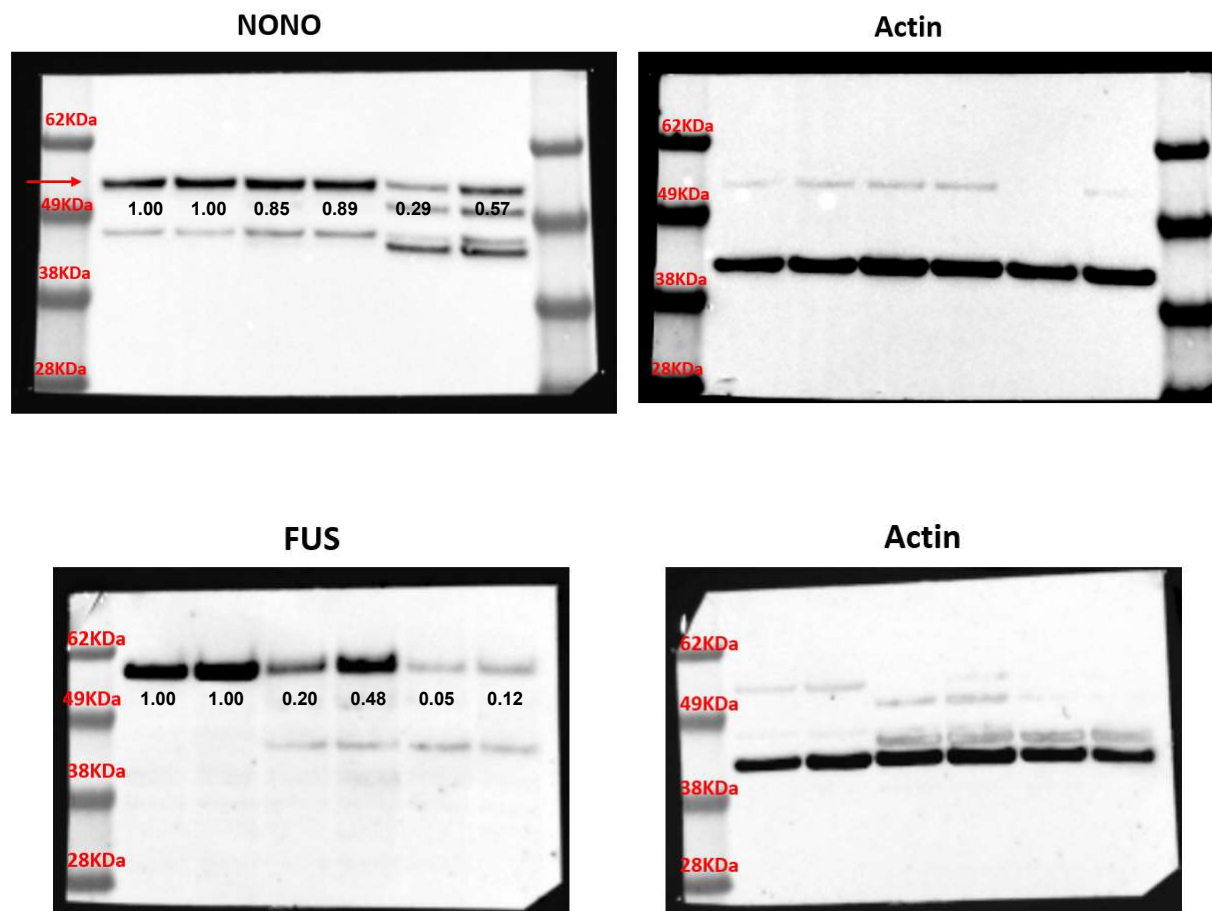


Figura 4F

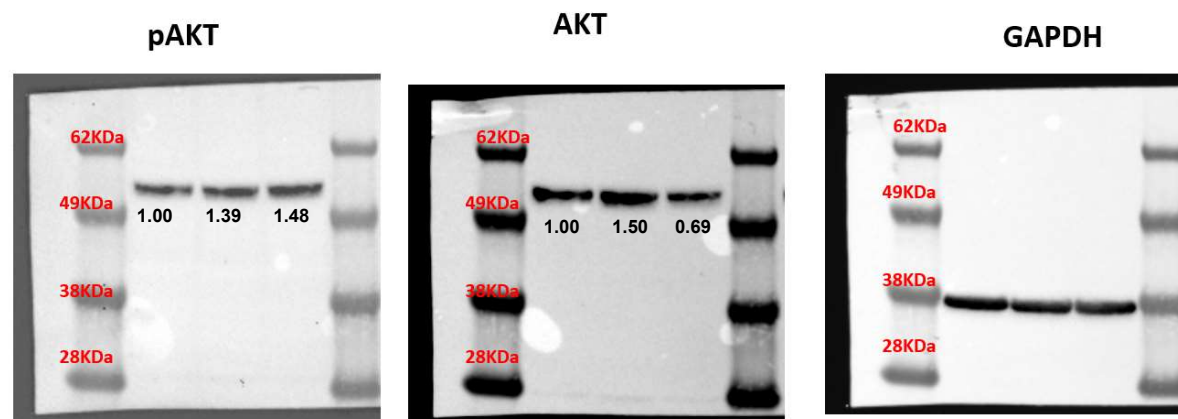
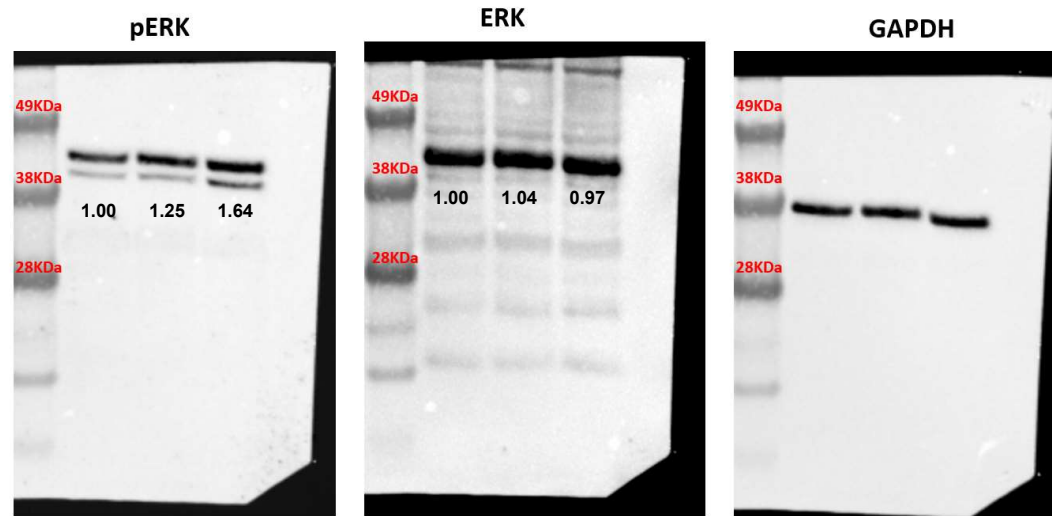


Figura 5A

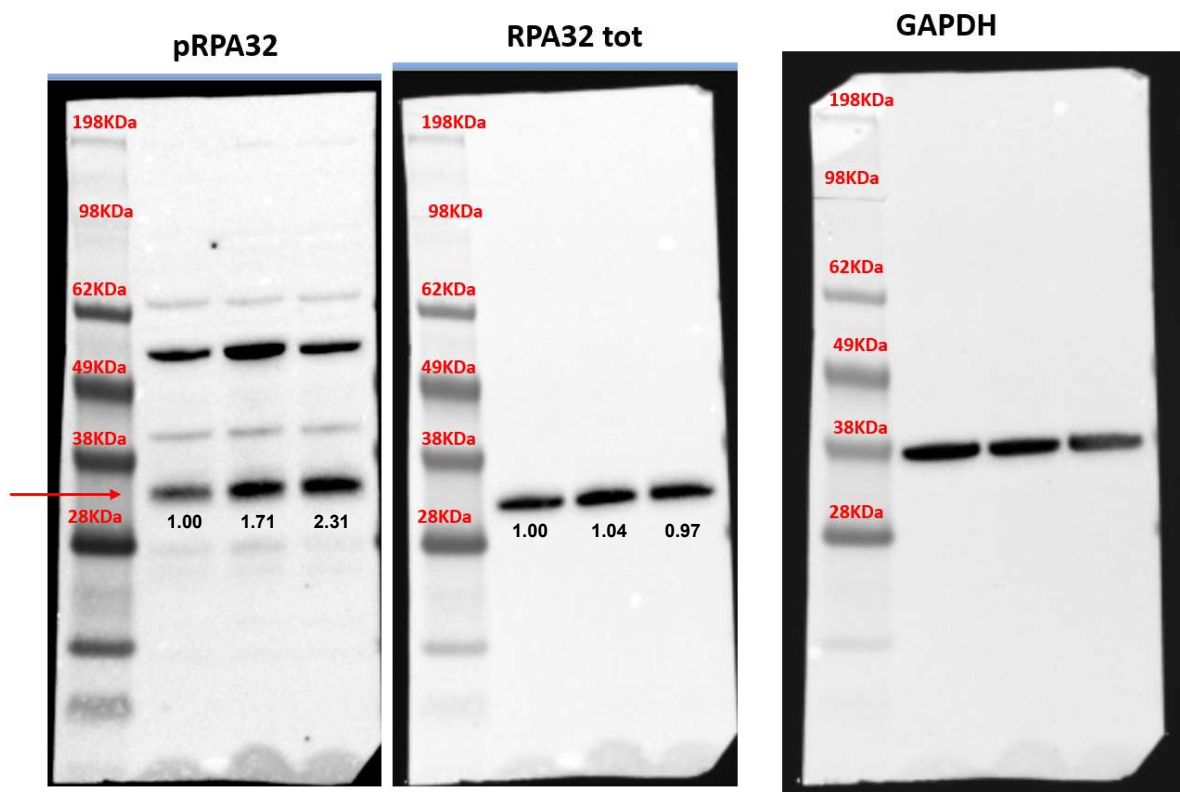


Figura 5C

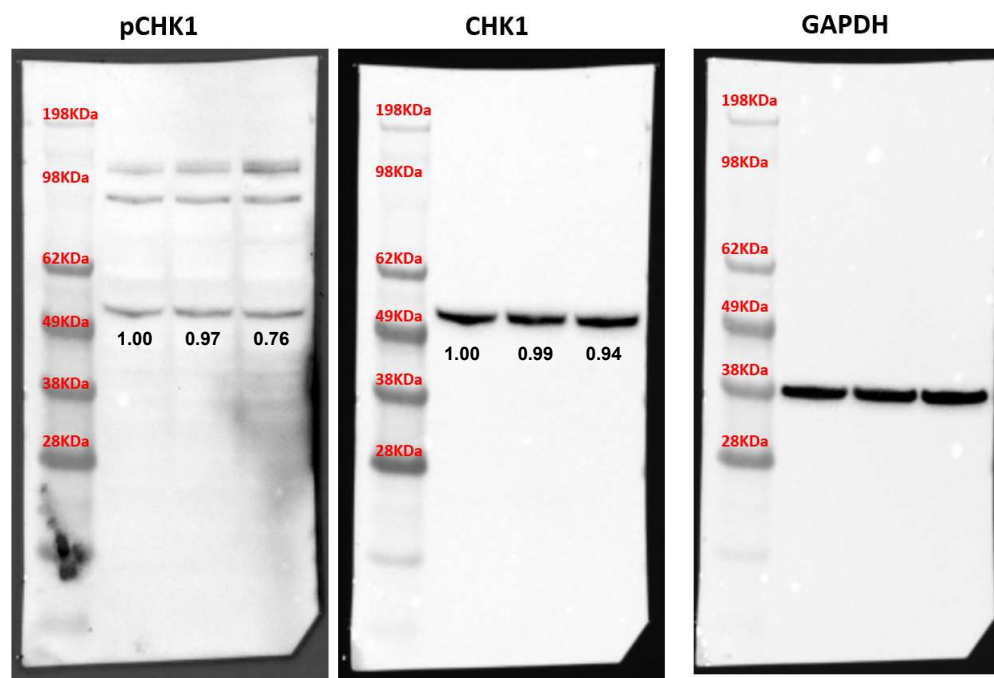
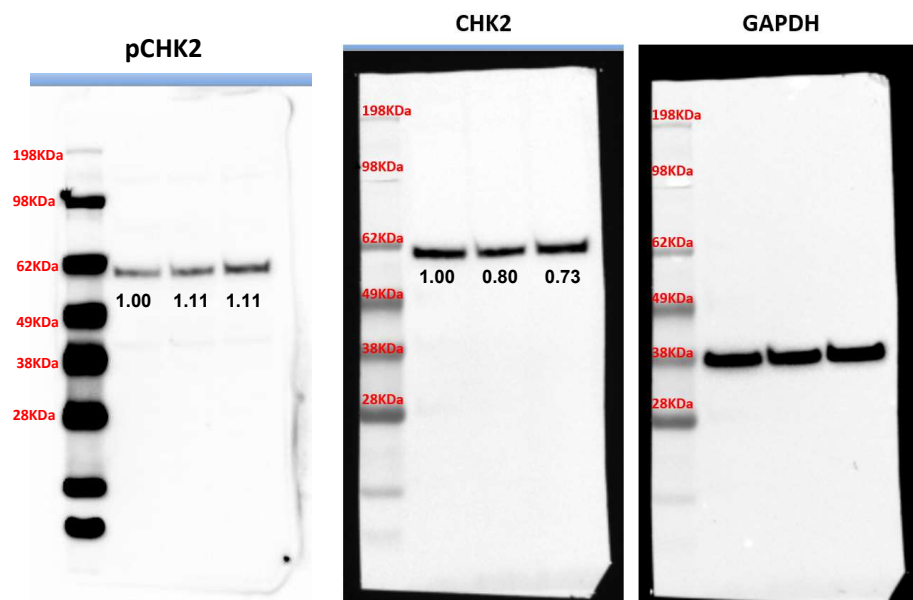


Figura 5D

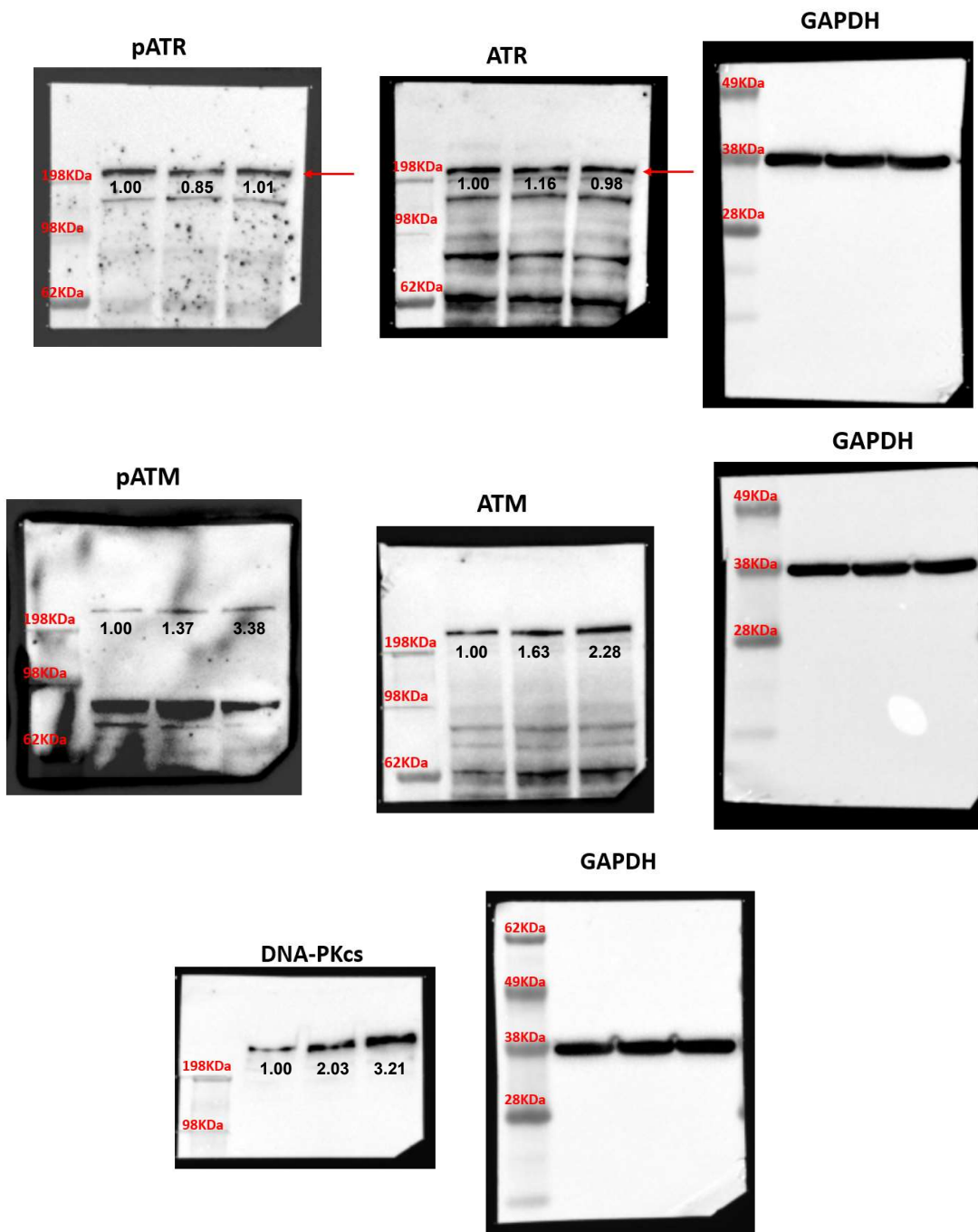


Figura 6B

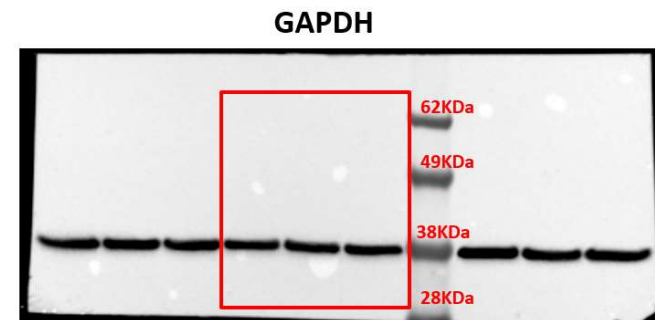
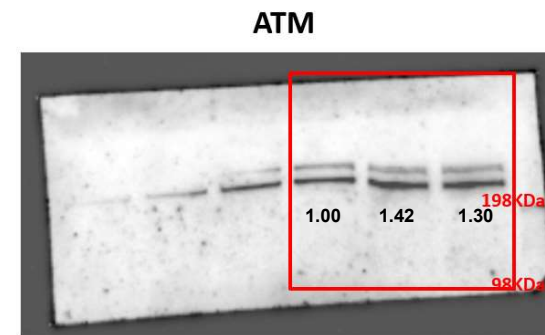
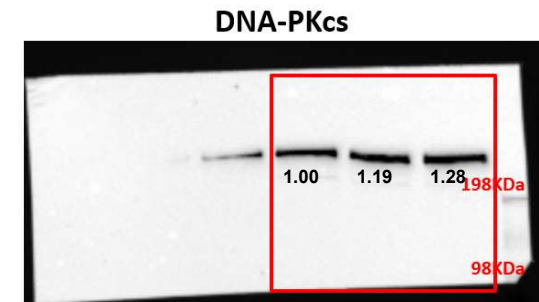
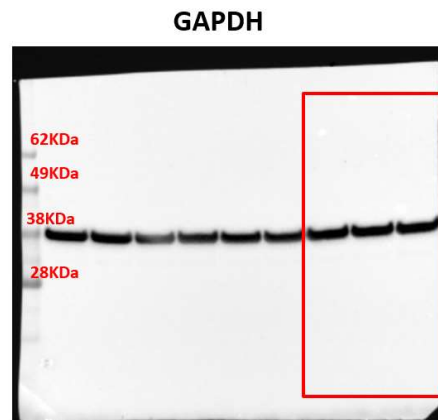
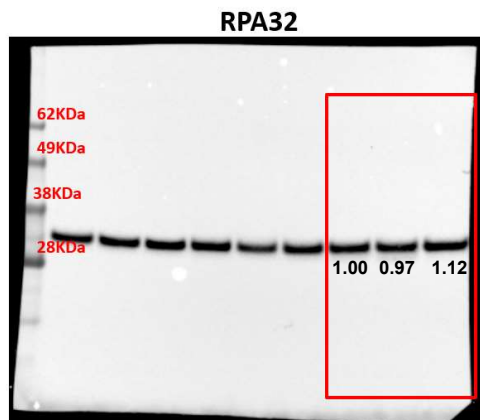
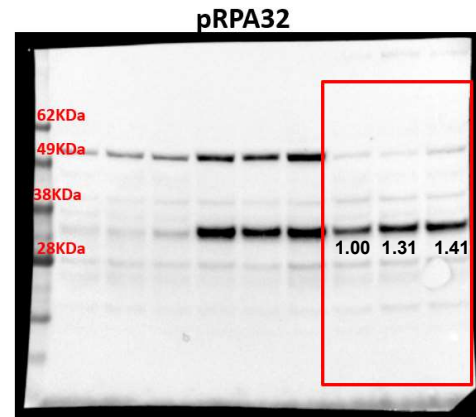


Figura 6C

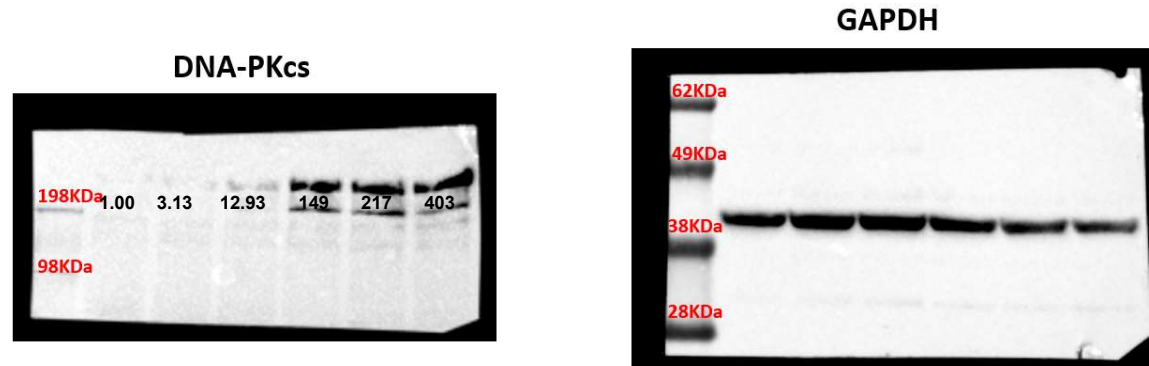


Figura 7B AMO1

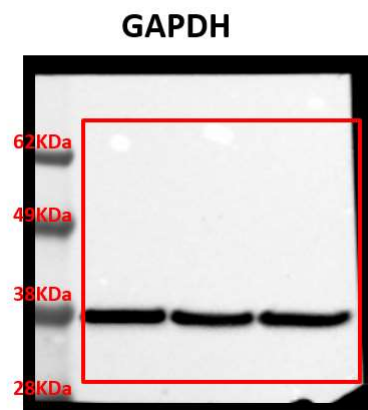
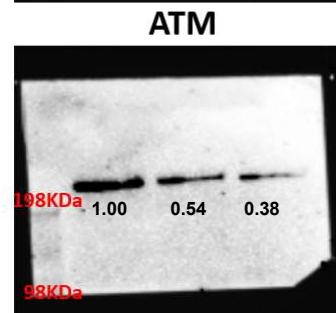
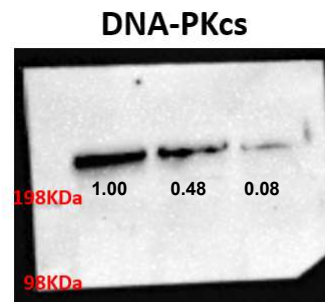
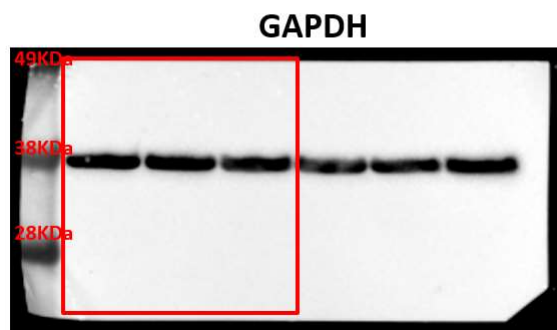
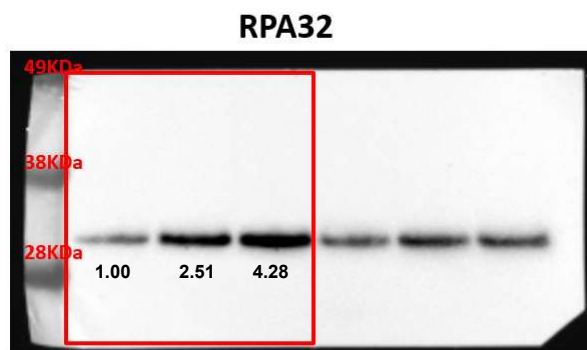
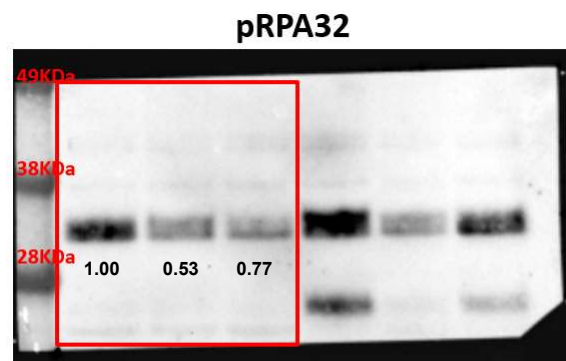
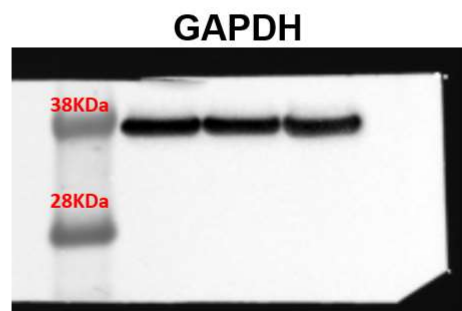
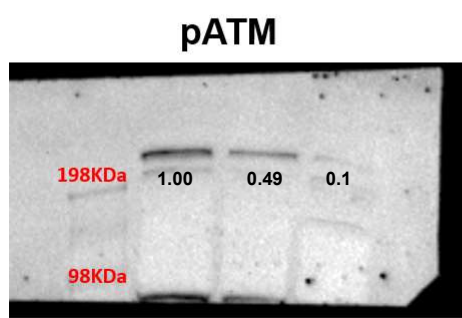
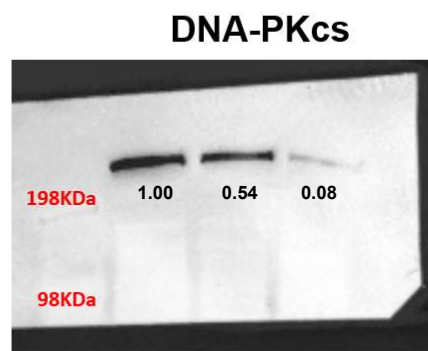
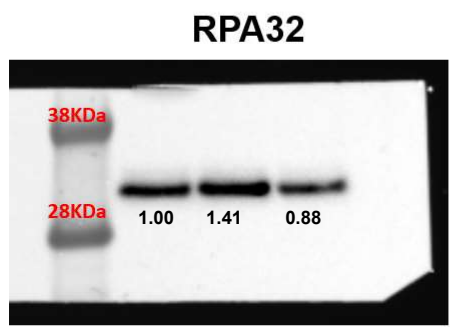
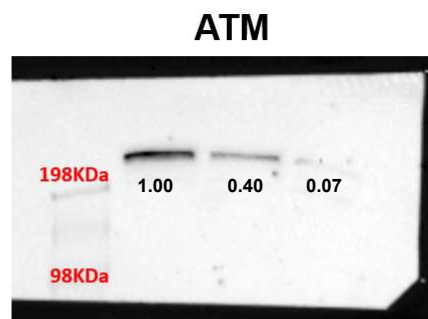
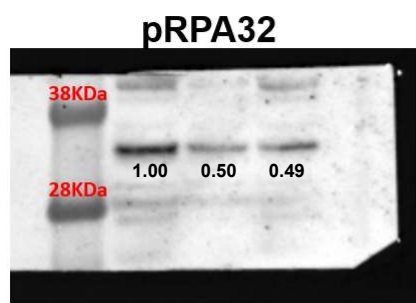
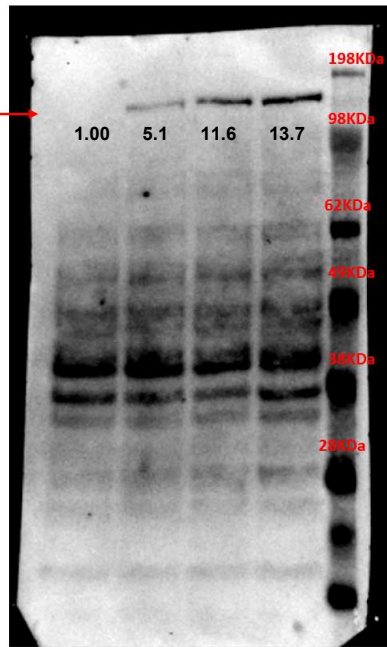


Figura 7B LP1

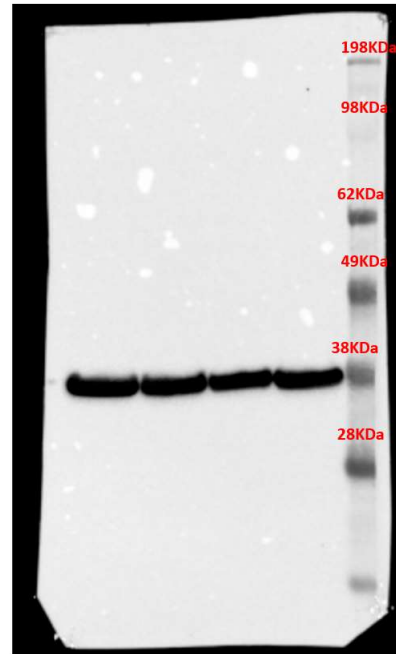


Supplementary Figure S1A

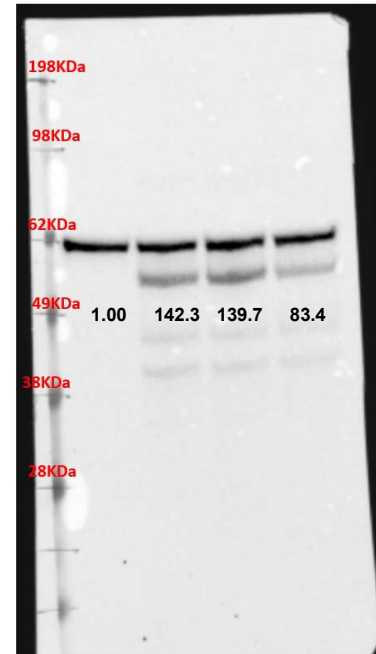
CAS9



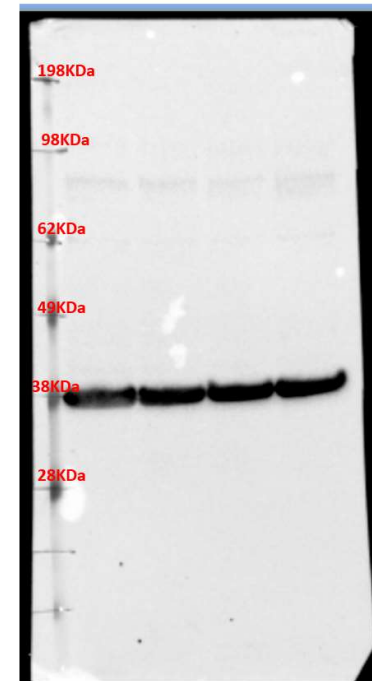
GAPDH



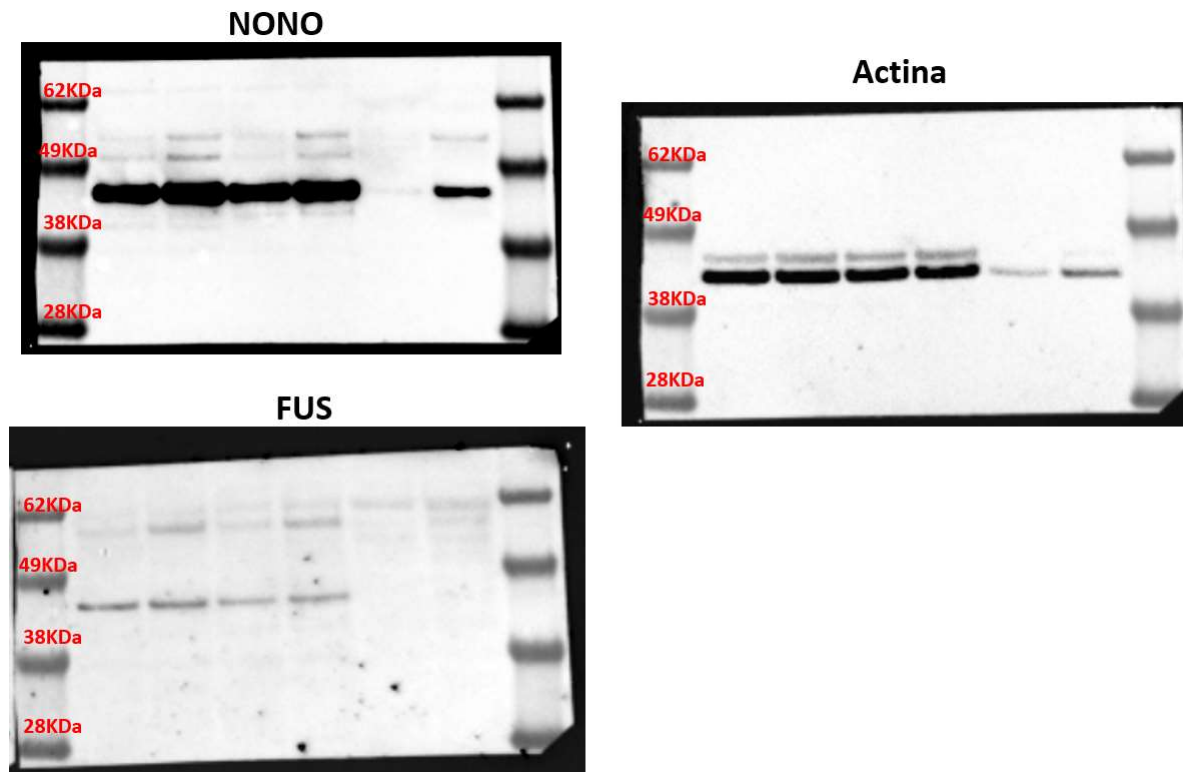
P65



GAPDH



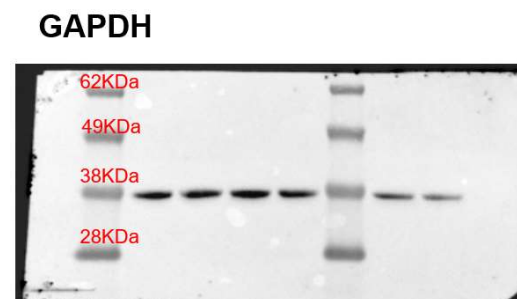
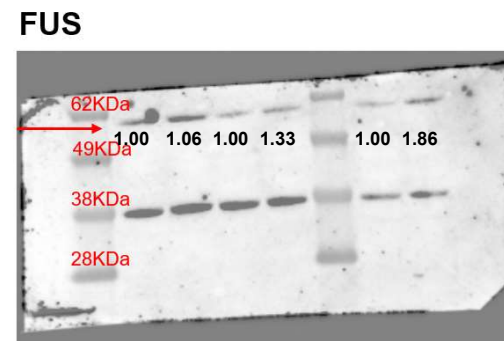
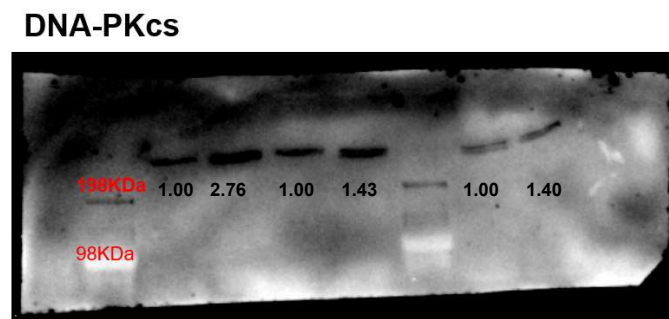
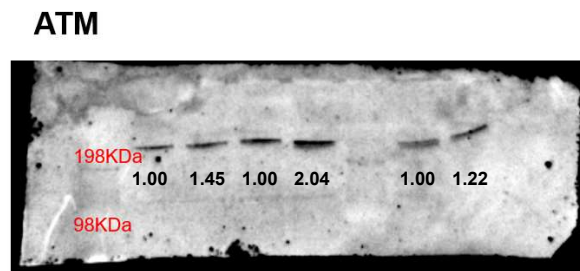
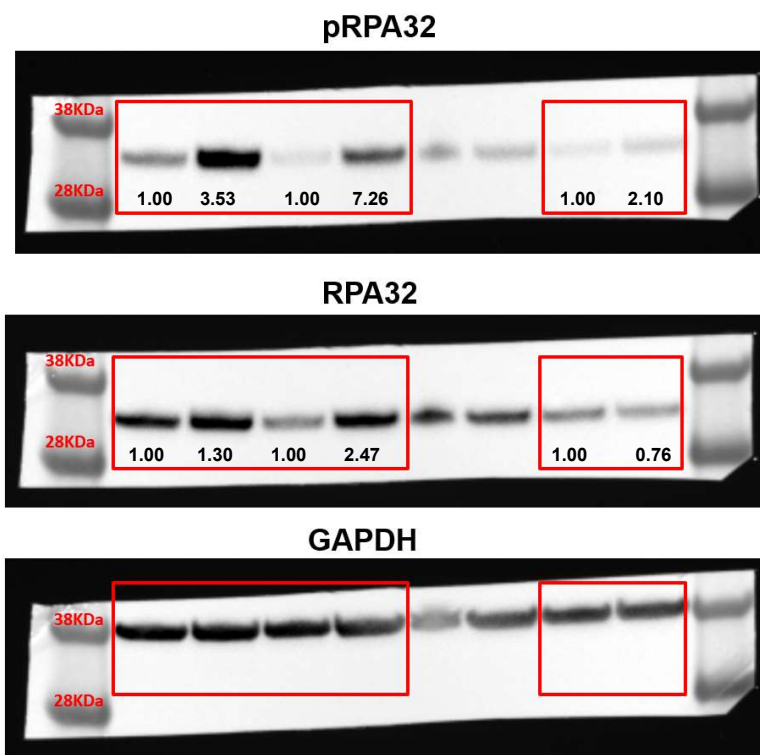
Supplementary Figure S3B



Supplementary Figure S7B

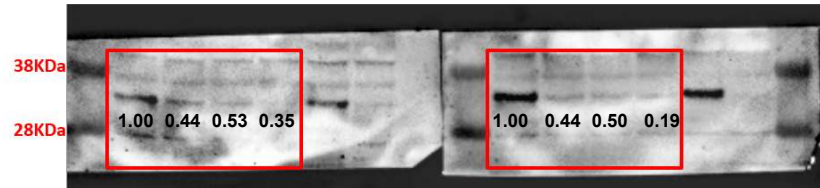


Supplementary Figure S9C

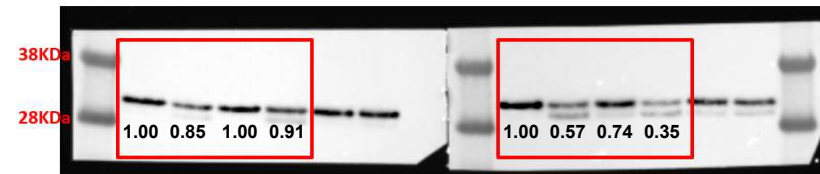


Suppl Figure S10A

pRPA32



RPA32



GAPDH

